Four-Element CPW-Fed UWB MIMO Slot Antenna with High Isolation and Triple Band-Notched Characteristics

Cheng-Zhu Du*, Zhi-Peng Yang, Hong-Ye Liu, and Yu Nie

Abstract—A novel 4-element UWB MIMO (multiple-input multiple-output) slot antenna with triple band-notched characteristics is designed and fabricated. It is composed of four rectangular slot antennas with two C-slots and a T-slot. To improve the isolation, cross-shaped branches are added. The measured results demonstrate that the antenna can operate ranging 2.51–11.07 GHz with the impedance bandwidth ($S_{11} < -10$ dB) of 856 MHz except three rejected bands, including 3.02–4.07 GHz, 4.54–5.83 GHz, and 7.88–9.38 GHz, and the inter-element isolation of antenna in the range of UWB band is higher than 21 dB. The presented antenna can filter the interference of WiMAX (3.3–3.7 GHz), WLAN (5.15–5.825 GHz) and X-band (7.9–8.4 GHz). Moreover, the parameters of diversity performance like envelope correlation coefficient (ECC), diversity gain (DG), efficiency, gain, channel capacity loss (CCL), mean effective gain (MEG), and total active reflection coefficient (TARC) have been analyzed. Based on the analysis on simulated and measured results, the proposed MIMO antenna is competent for UWB applications with notched bands for WiMAX, WLAN and X-band.

1. INTRODUCTION

Since the US Federal Communication Commission (FCC) announced the ultra-wideband (UWB) from 3100 MHz to 10600 MHz in 2002 [1, 2], UWB technology has attracted extensive public attention. UWB technology is widely used in image, radar, communications, and other fields [3, 4]. Meanwhile, the technology of multiple-input multiple-output (MIMO) can greatly improve the channel capacity and the quality of wireless communication without additional transmission power and spectrum resources, so it has become a research hot point in wireless communication [5–7]. Therefore, it is crucial to combine MIMO and UWB technologies to realize their advantages. There are many narrowband communication frequency bands in the UWB, such as WiMAX, WLAN, and X-band communication satellites [8]. Undoubtedly, UWB antennas with band-notch characteristics can suppress the interference from narrowband signals.

UWB antennas with band-notch characteristics have been presented in [9–18]. In [9], a two-element MIMO antenna with UWB performance is presented, and a T-shaped strip is loaded at the middle of antenna to improve isolation. In [10], a new compact UWB-MIMO antenna with band notch characteristics is presented for wireless application. It comprises two unique monopole antenna elements sharing a similar ground plane. In [11], a UWB-MIMO antenna consists of two shared circular radiators with dual band-notched characteristics. In [12], a CPW-fed MIMO-UWB antenna with dual band-notched characteristic is proposed with high isolation by adopting a double Y-shaped branch between the two radiation elements. A triple band-notched MIMO antenna with decoupling network is described in [13], Electromagnetic Band Gap (EBG) structure is used to filter the signals of WiMAX

* Corresponding author: Cheng-Zhu Du (duchengzhu@163.com).
The authors are with the College of Electronics and Information Engineering, Shanghai University of Electric Power, Shanghai 200090, China.

and WLAN bands. In [14], It proposes a CPW-fed four-port rectangular monopole antenna for UWB-MIMO applications. By etching step on the ground plane and arrow-shaped on the radiating patch, the bandwidth and performances have been promoted. In [15], a compact polygon shaped 4-element antenna with band notched characteristics is presented using Koch geometry, achieving high isolation. In [16], a four-element MIMO antenna obtain band rejection phenomenon by etching an elliptical CSRR slot. In [17], a four-element MIMO system with dual band-notched characteristic is proposed, loaded with complementary split ring resonator for eliminating the WLAN and WiMAX bands. A four-element UWB-MIMO antenna using integration technology is presented in [18], which achieves higher isolation by using orthogonal structure, and different types of slots are inserted in the radiating elements to generate three notched bands. Most of the above antennas are fed by microstrip, which can not be used easily in integrated circuits [19].

A 4-element co-planar waveguide (CPW) fed UWB MIMO slot antenna with triple band-notched characteristic is printed on an FR4 substrate in this article. The antenna elements are arranged vertically, and cross-shaped branches are added to improve the isolation of more than 21 dB. The innovations of proposed antenna include (1) the feeding line of CPW makes it easier with integrated microwave circuit; (2) the 4-element MIMO antenna can filter the interference of unwanted signals with triple band-notched characteristic; (3) the slot antenna has good characteristic of wide impedance matching.

2. ANTENNA DESIGN

2.1. Single Element Antenna

The geometrical details of the single element antenna are depicted in Figure 1(a), and Figure 1(b) shows the S_{11} of single element antenna. The antenna is printed on an FR4 dielectric substrate with an overall size of $22\,\text{mm} \times 30\,\text{mm} \times 0.8\,\text{mm}$, a relative dielectric constant of 4.4, and a loss tangent of 0.02. The single element antenna is composed of a rectangle radiator with two C-slots and a T-slot, operating from 2.9 to 11.3 GHz with tri-band rejection characteristics, which can eliminate the interference of WiMAX, WLAN, and X-band. The length of the slot is usually $\frac{\lambda}{4}$ as follows:

$$L = \frac{C}{4 f_c \cdot \sqrt{\varepsilon_{\text{eff}}}} \tag{1}$$

Table 1 gives the details of antenna parameters.

Figure 2(a) shows the design procedure of single element antennas from Ant 1 to Ant 4. Figure 2(b) shows the S_{11} of four different antennas. It can be seen that the inner C-slot can filter the influences of

(a)   (b)
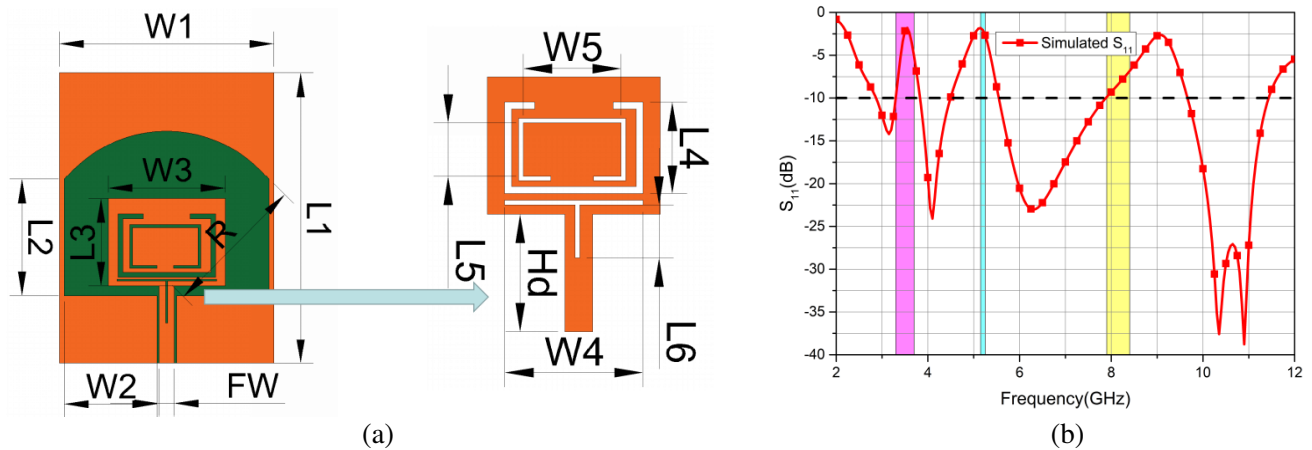
Figure 1. Structure and S_{11} of proposed single element antenna. (a) Structure of single element antenna. (b) S_{11} of single element antenna.

Table 1. Optimized design parameters and dimensions of the single element antenna (unit: mm).

L1	L2	L3	L4	L5	FW	R
30	12	9	6.5	4.5	1.56	15
W1	W2	W3	W4	W5	Hd	L6
22	9.5	12	10	7.3	8	4

(a)

(b)
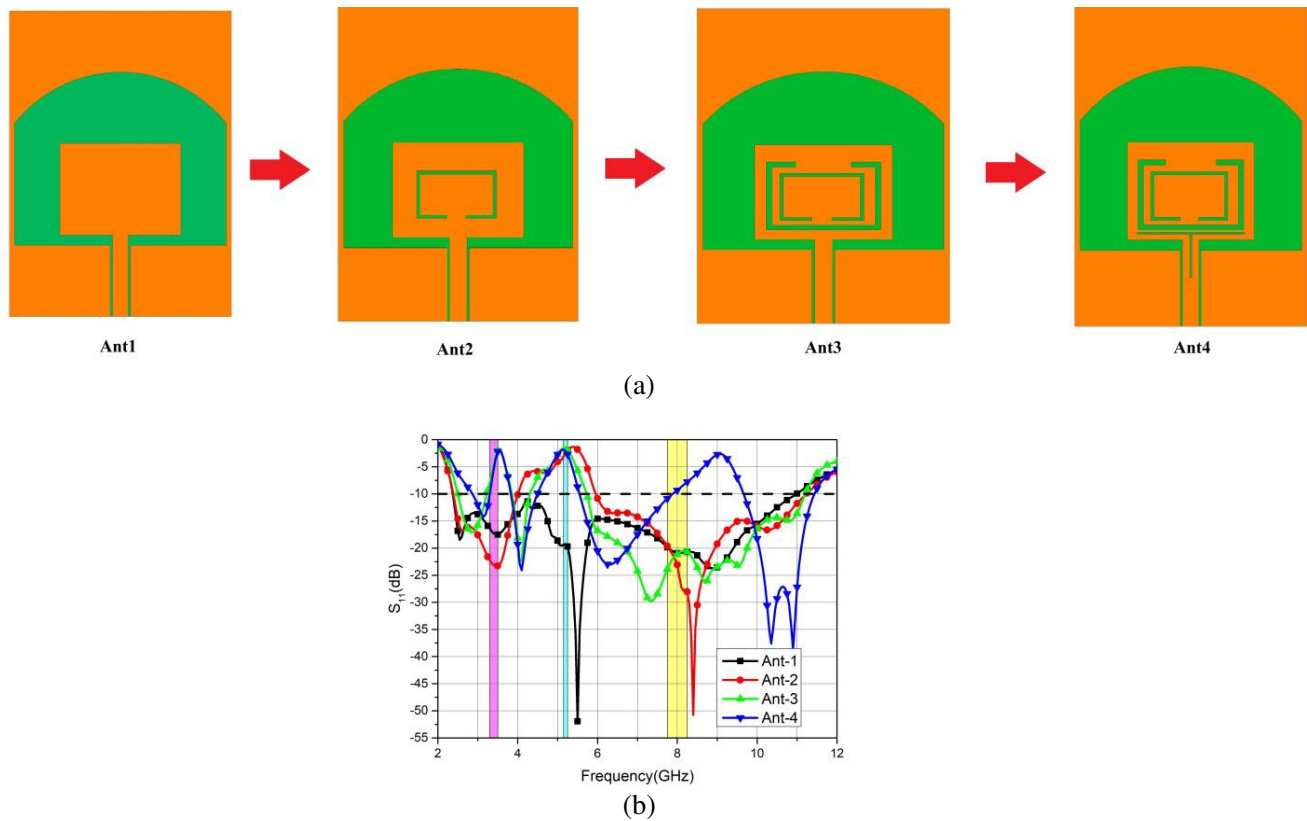
Figure 2. The design procedure and the S_{11} of four different antennas. (a) Design procedure. (b) The S_{11} curves of different antennas in design procedure.

WiMAX systems; the outer C-slot can filter the influences of WLAN systems; and the T-slot generates a notch band of 7.9–9.6 GHz corresponding to X-band systems.

Figure 3 presents the parameters analysis of the slots with various $L4$ and $L6$. It is shown in Figure 3(a) that the first notched band at the lower band is shifted to lower frequency, when the length of $L4$ increases. In Figure 3(b), with the extension of the length of $L6$, the notched band at the higher band is shifted to lower frequency, while the other two notched bands are nearly unaffected.

2.2. Four-Element MIMO Antenna

The four-element CPW-fed MIMO slot antenna with triple notched bands is proposed. The antenna is printed on an FR4 substrate with dimensions $65\,\text{mm} \times 65\,\text{mm} \times 0.8\,\text{mm}$. In order to realize the compactness of the antenna, the isolation structure of the antenna is placed obliquely between antenna elements, and the θ is $5°$. The length of the isolation structure Lf is $60\,\text{mm}$. The structure and photo of the antenna are displayed in Figure 4.

(a)   (b)
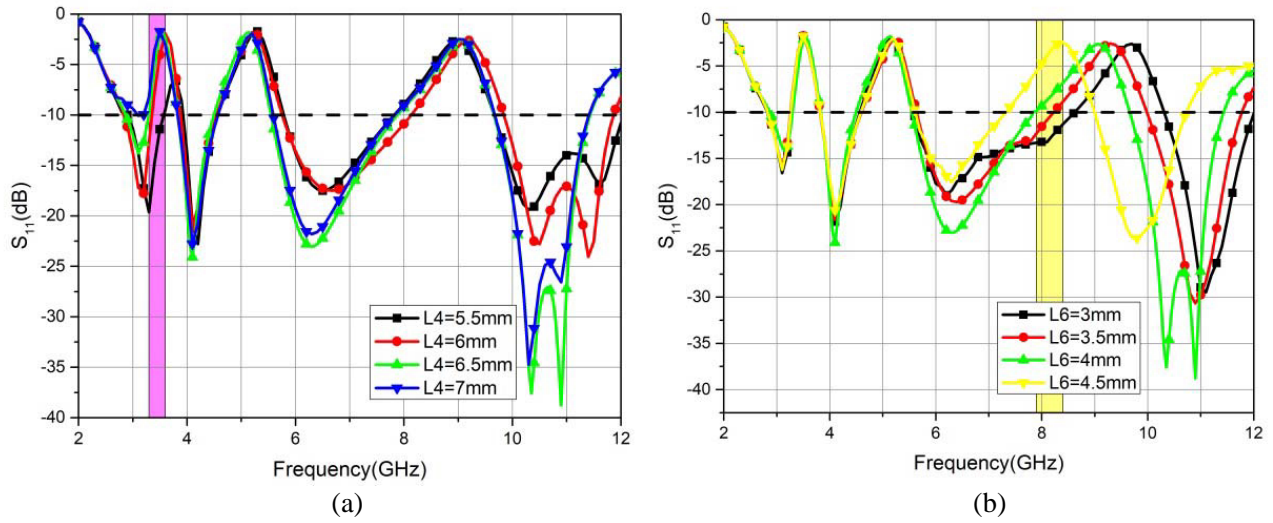
Figure 3. Simulated S_{11} of the proposed MIMO antenna for various $L4$ and $L6$. (a) $L4$, (b) $L6$.

(a)   (b)
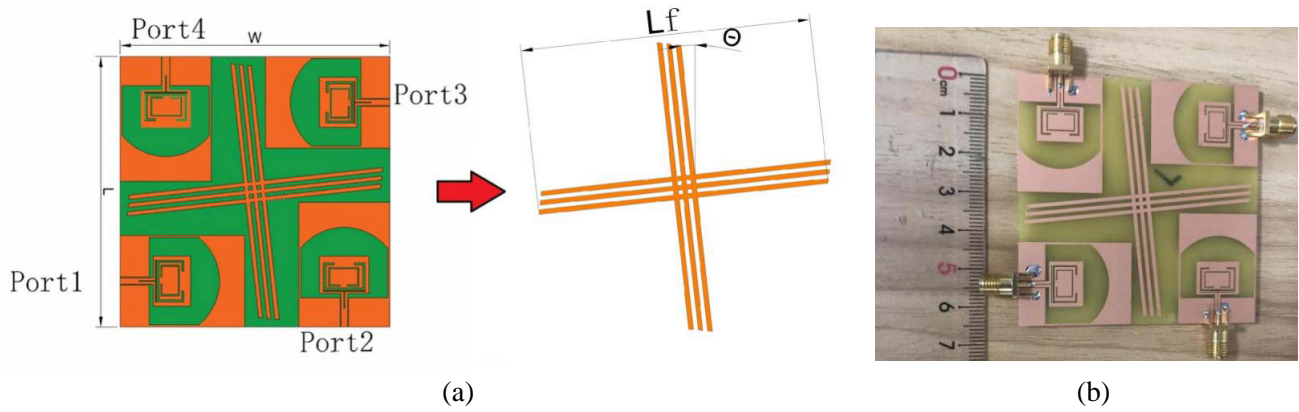
Figure 4. The proposed UWB-MIMO antenna. (a) Geometric structure of the antenna. (b) Fabricated antenna.

(a)   (b)
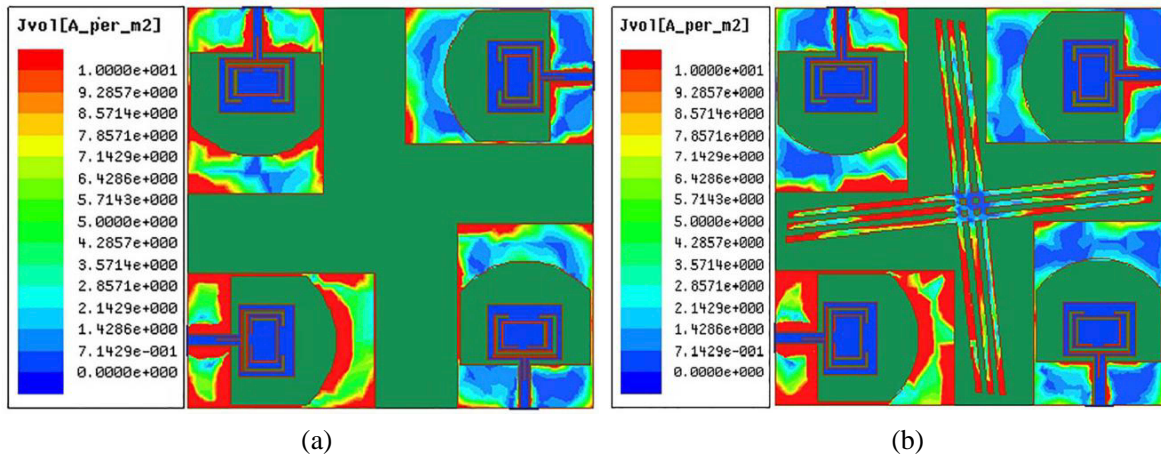
Figure 5. The current distributions of the antenna with and without isolation structure. (a) Without isolation structure. (b) With isolation structure.
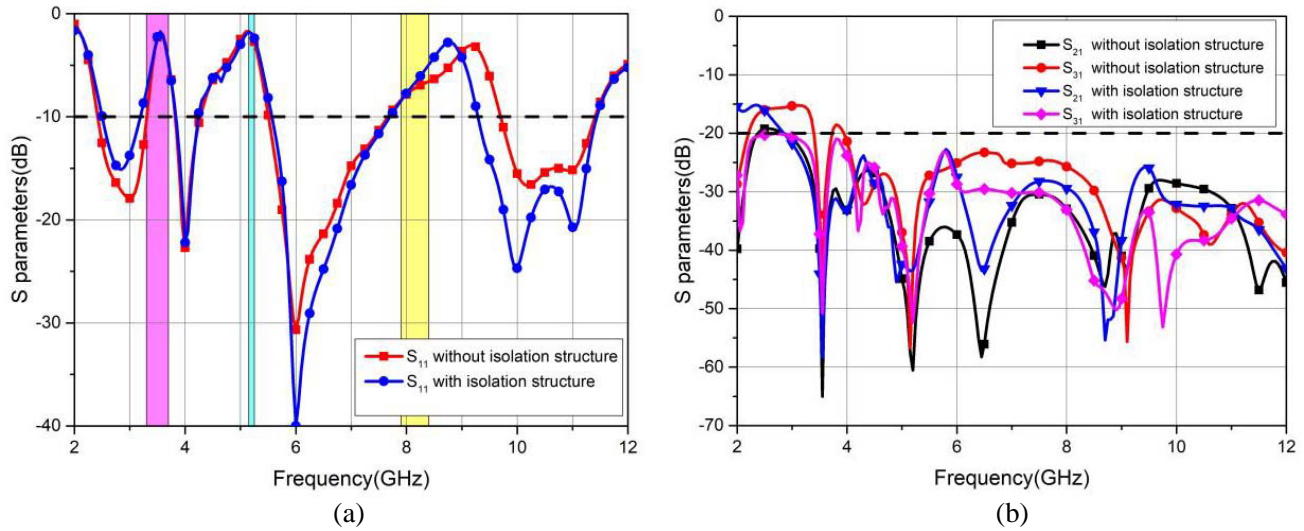
Figure 6. The S parameters of the antenna with and without isolation structure. (a) S_{11} with and without isolation structure. (b) S_{21} with and without isolation structure.

In order to have a better intuitive sight of the electromagnetic mechanism, the current distributions of proposed antenna with and without the isolation structure at 6 GHz are shown in Figure 5. In Figure 5(a), the antenna without isolation structure has poor isolation, and a lot of current flows from excited port 1 to other ports at 6 GHz. In Figure 5(b), by adding the isolation structure, the mutual coupling current is significantly reduced, which proves that the isolation branches prevent the current from port 1 flowing to other antenna elements. Figure 6 shows the S parameters of the antenna with and without isolation structure. After adding isolation branches on the antenna, it is observed that the simulated S_{31} has been significantly improved in all working bands, and the simulated S_{21} have become a little worse below 2.8 GHz frequencies.

Because the isolation branches are mainly effective to improve the S_{31} of the antenna in the lower frequency band (2–3.5 GHz), the S_{31} of the antenna is analyzed. Figure 7 displays the simulated S_{31} without and with different numbers of isolation branches. It can be seen that S_{31} is less than -20 dB at all bands, when the number of branches is 3.
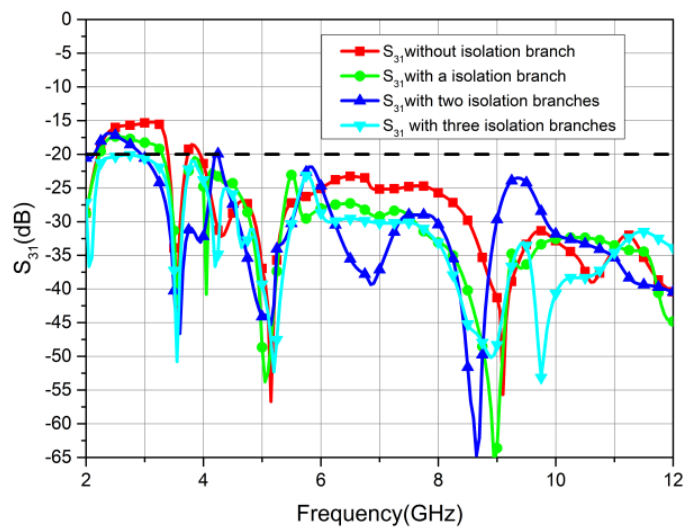
Figure 7. The simulated S_{31} with different branches.

3. EXPERIMENTING VERIFICATION

3.1. *S*-Parameter

The reflection coefficients are derived by allowing port 1 excited and other ports matched with 50-Ω load. Figure 8 presents simulated and measured results of S-parameters including S_{11}, S_{22}, S_{33}, S_{44}, S_{21}, S_{31}, and S_{41} in comparison with simulated results, and the trend of measured results is the same as that of simulated ones. The measured antenna achieved a wide impedance bandwidth of 8.56 GHz ranging 2.51–11.07 GHz with three reject bands at 3.02–4.07 GHz, 4.54–5.83 GHz, and 7.88–9.38 GHz, which effectively filters the WiMAX (3.3–3.7 GHz), WLAN (5.15–5.25 GHz, 5.725–5.825 GHz), and X-band (7.9–8.4 GHz). Figure 8(b) shows that the measured port isolation is lower than -21 dB, which is much higher than the requirement of MIMO antennas.
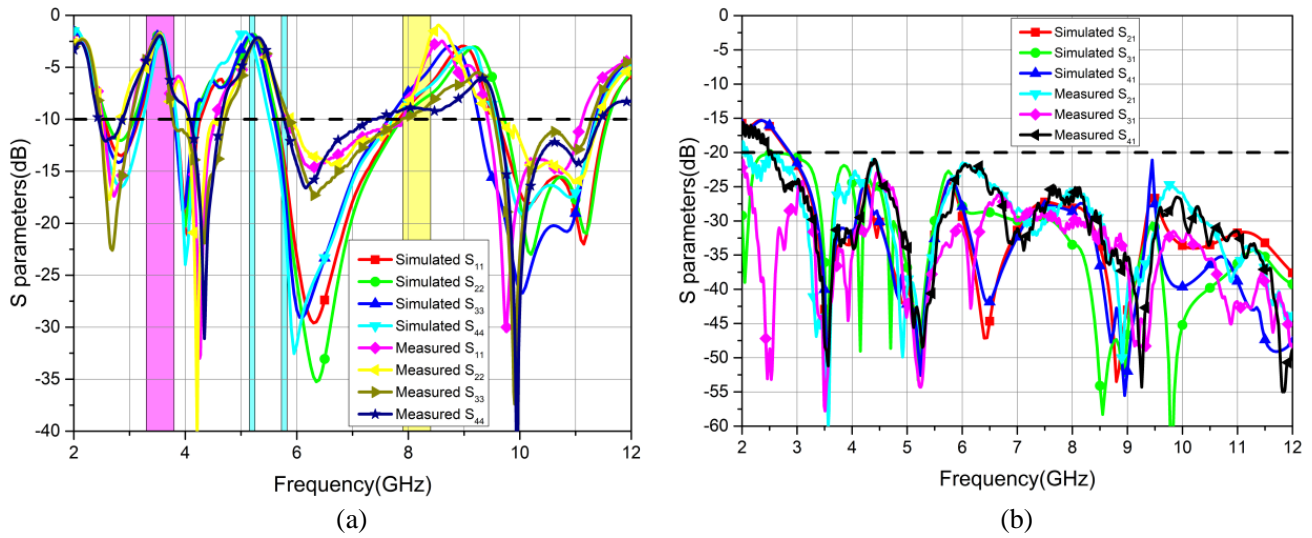
Figure 8. Simulated and measured S-parameters of the MIMO antenna. (a) S_{11}, S_{22}, S_{33} and S_{44}. (b) S_{21}, S_{31} and S_{41}.

(a)
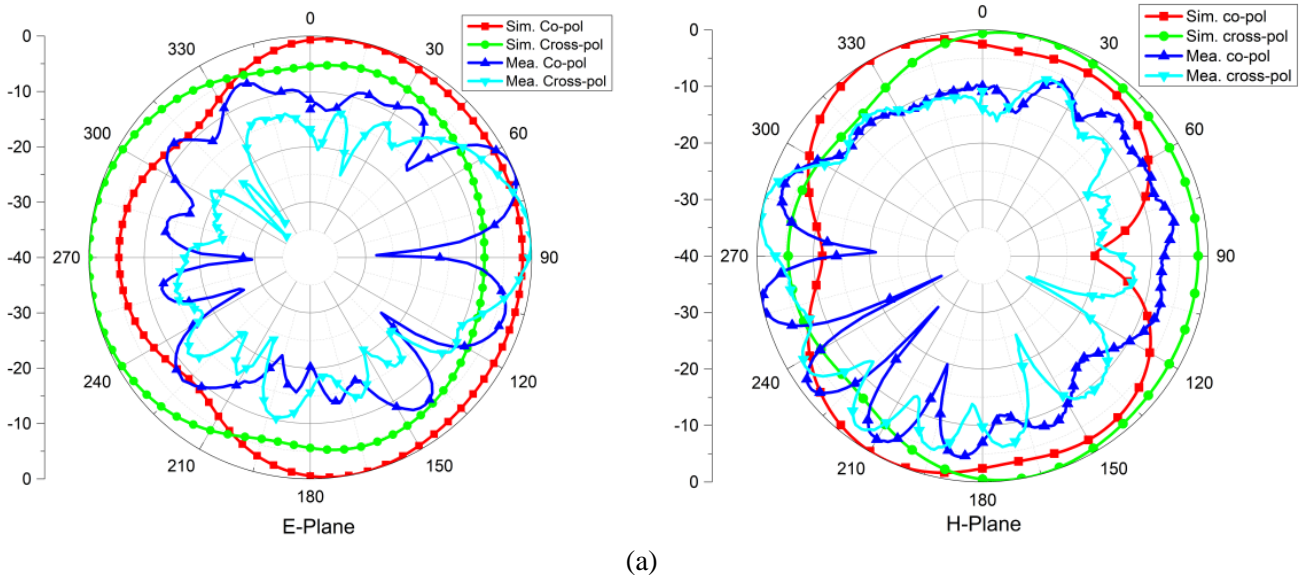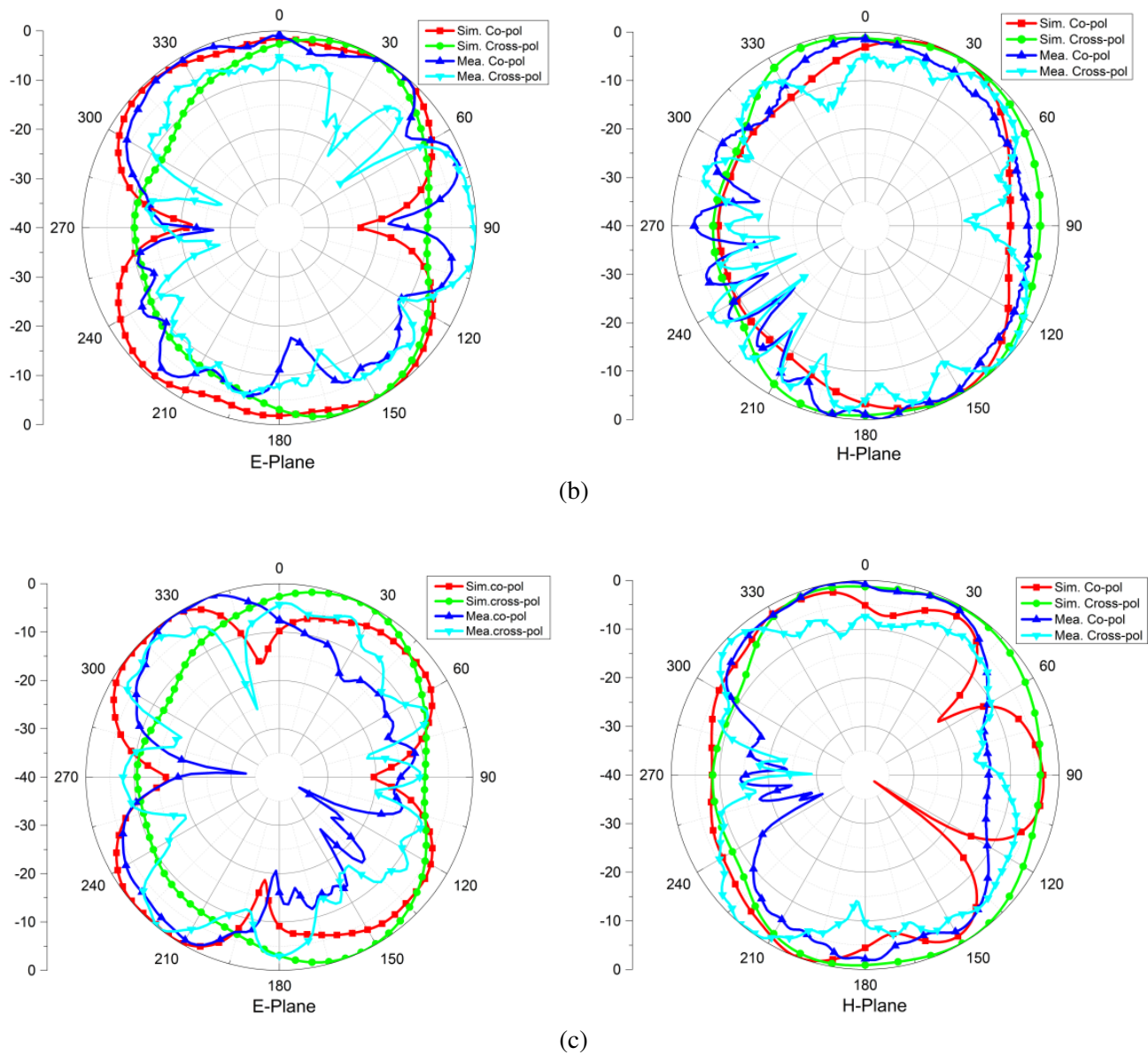
Figure 9. Simulated and measured radiation patterns of the MIMO antenna. (a) 4 GHz, (b) 6 GHz, (c) 10 GHz.

3.2. Radiation Pattern

The co-polarization and cross-polarization of proposed antenna are simulated and measured in E-plane and H-plane. The bidirectional and omnidirectional patterns at 4 GHz, 6 GHz, and 10 GHz have been plotted in Figure 9. The level of cross-polarization is below the co-planar polarization at some points, when compared with the co-planar polarization. It can be demonstrated from the measured results that the antenna meets the design requirements. On account of the uncertainty of testing environment and fabrication tolerance, the measured results are slightly different from the simulated ones.

4. DIVERSITY PERFORMANCE

4.1. Gain and Efficiency

Figure 10 presents the curves of gains and radiation efficiency. It is shown that the simulated and measured gains both have triple band-notched characteristics, and the maximum gain is 5 dB. The measured gain is slightly weaker than the simulated one at some frequencies, which generally attributes to the uncertainty of the measurement environment and the loss of the SMA connector. The radiation efficiency is more than 95% in the working frequency bands.
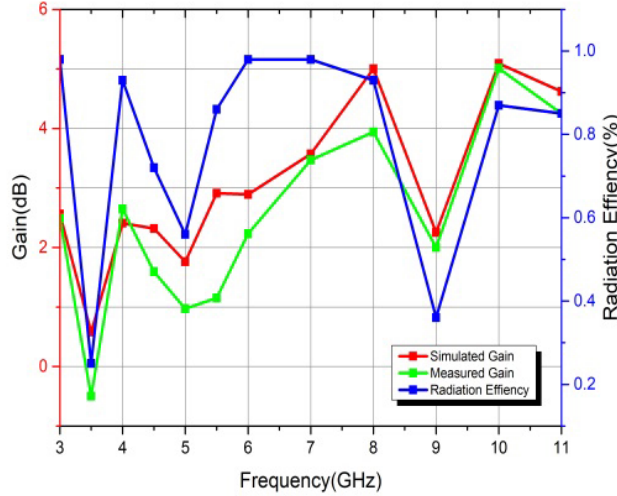
Figure 10. Gain and radiation efficiency of the MIMO antenna.

4.2. Envelope Correlation Coefficient and Diversity Gain

The parameter, envelope correlation coefficient (ECC), is crucial to estimating the extent of correlation between elements in a MIMO system. The ECC can be calculated approximately as follows [20]:

$$\rho_e\left(i, j, N\right) = \frac{\left|\sum_{n=1}^{N} S_{i,n}^* S_{n,j}\right|^2}{\prod_{k=(i,j)}\left[1 - \sum_{n=1}^{N} S_{i,n}^* S_{n,k}\right]} \tag{2}$$

Similarly, when the characteristics of MIMO antenna are evaluated, diversity gain (DG) is also crucial, which can be calculated by the following equation [21]:

$$\text{DG} = 10\sqrt{1 - (\text{ECC})^2} \tag{3}$$

As shown from Figure 11, the value of measured ECC is lower than 0.005. Figure 12 shows the simulated and measured DGs for each element. Measured DG is better than 9.998 within operating band, confirming that the proposed antenna has good diversity.

4.3. Channel Capacity Loss and Mean Effective Gain

Channel capacity loss (CCL) is often used to examine diversity performance, describing how fast the constant message transmission rate can be achieved. Good diversity performance for MIMO antenna requires CCL below 0.4 bits/s/Hz within operating band. We can obtain CCL of a MIMO antenna with four elements by the following equation:

$$\text{CCL} = -\log_2\det(\alpha^R) \tag{4}$$
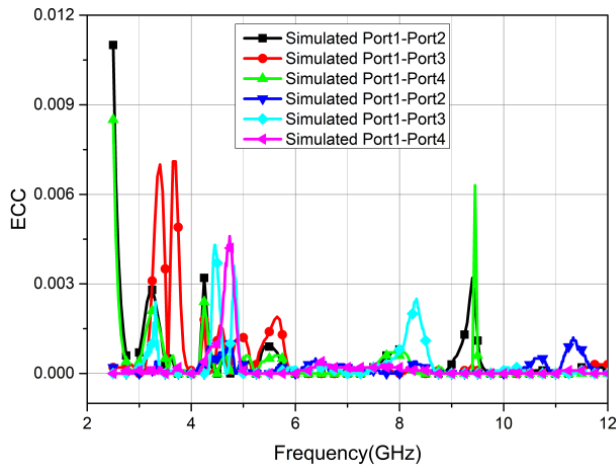
Figure 11. ECC of the purposed antenna.
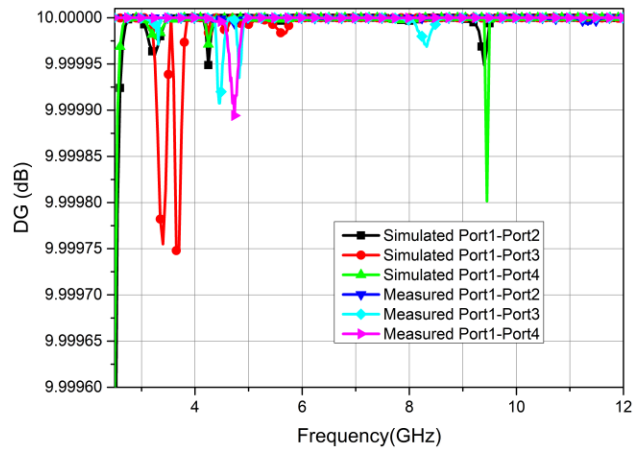
Figure 12. DG of the purposed antenna.

where $\alpha^R = \begin{bmatrix} \alpha_{11} & \alpha_{12} \\ \alpha_{21} & \alpha_{22} \\ \alpha_{13} & \alpha_{14} \\ \alpha_{23} & \alpha_{24} \\ \alpha_{31} & \alpha_{32} \\ \alpha_{41} & \alpha_{42} \\ \alpha_{33} & \alpha_{34} \\ \alpha_{43} & \alpha_{44} \end{bmatrix}$, $\alpha_{ii} = 1 - \left(\sum_{j=1}^{N} |S_{ij}|^2\right)$ and $\alpha_{ij} = -(S_{ii}^* S_{ij} + S_{ji}^* S_{ij})$.

The CCL curves are presented in Figure 13, which demonstrates that CCL in the working bands is lower than requirements.

At the same time, the mean effective gain (MEG) is used for the measurement of MIMO antenna characteristics. We can calculate MEG by the equation [22]:

$$\text{MEG}_i = 0.5 \left[1 - \sum_{J=1}^{N} |S_{ij}|^2 \right] \tag{5}$$

$$|\text{MEG}_i - \text{MEG}_j| < 3\,\text{dB} \tag{6}$$
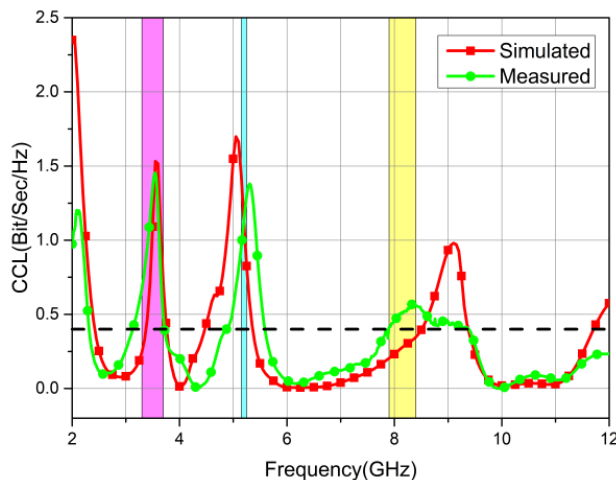
Figure 13. CCL of the purposed antenna.
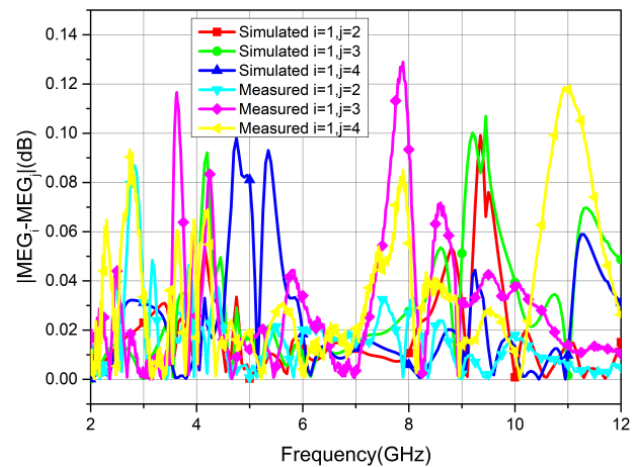
Figure 14. MEG of the proposed antenna.

Generally, the difference between MEG_i is allowed to be below 3 dB. Figure 14 plots curves of the difference between MEGs, showing that the value is less than 0.13 dB in UWB, which indicates that the proposed MIMO antenna totally meets the requirements.

4.4. Total Active Reflection Coefficient

The total active reflection coefficient (TARC) is regard as a basic parameter to predict the overall MIMO system behavior. The value of TARC is expressed as [23]:

$$\text{TARC} = N^{-0.5} \sqrt{\sum_{i=1}^{N} \left| \sum_{k=1}^{N} S_{ik} e^{j\theta_{k-1}} \right|^2} \tag{7}$$

where N denotes the number of antennas, and θ is the input feeding phase. The curves of the TARC are shown in Figure 15. TARC is lower than -10 dB at UWB except three rejected bands, demonstrating that the proposed antenna is desirable for MIMO application.

4.5. Performance Comparison

A comparison between the antenna proposed in this paper and previous reported antennas is shown in Table 2. As observed from the table, the proposed CPW-fed slot antenna has the advantages of a broader bandwidth, a lower ECC, and an enhanced isolation. In addition, the CPW-fed MIMO antenna is easily connected to the integrated circuits.

Table 2. Performance comparison with previous MIMO antennas.

Ref.	Bandwidth (GHz)	Effective area (mm)	Isolation (dB)	Port	Notches	ECC	DG	Feeder method
[9]	3.08–11.8 (117%)	$\lambda_0 \times \lambda_0$	< -15	2	1	< 0.02	-	Microstrip feed
[10]	3.1–20 (146%)	$0.7\lambda_0 \times \lambda_0$	< -18	2	1	< 0.3	9.95	Microstrip feed
[11]	2.9–12 (122%)	$1.2\lambda_0 \times 1.2\lambda_0$	< -15	2	2	< 0.15	-	Microstrip feed
[12]	2.36–12 (134%)	$1.2\lambda_0 \times 1.2\lambda_0$	< -21	2	2	< 0.04	9.9	CPW feed
[13]	2–11 (138%)	$1.4\lambda_0 \times \lambda_0$	< -15	2	3	< 0.02	-	Microstrip feed
[14]	3.1–10.6 (109%)	$1.8\lambda_0 \times 1.8\lambda_0$	< -17	4	0	< 0.001	-	CPW feed
[15]	2–10.6 (130%)	$\lambda_0 \times \lambda_0$	< -17	4	1	< 0.5	-	Microstrip feed
[16]	3–13.5 (127%)	$1.6\lambda_0 \times 1.6\lambda_0$	< -22	4	2	< 0.008	9.98	Microstrip feed
[17]	3–14 (129%)	$1.3\lambda_0 \times 1.3\lambda_0$	< -20	4	2	< 0.01	9.95	Microstrip feed
[18]	2.3–13.75 (142%)	$\lambda_0 \times \lambda_0$	< -22	4	3	< 0.02	9	Microstrip feed
Prop	2.51–11.07 (126%)	$1.4\lambda_0 \times 1.4\lambda_0$	< -21	4	3	< 0.005	9.998	CPW feed
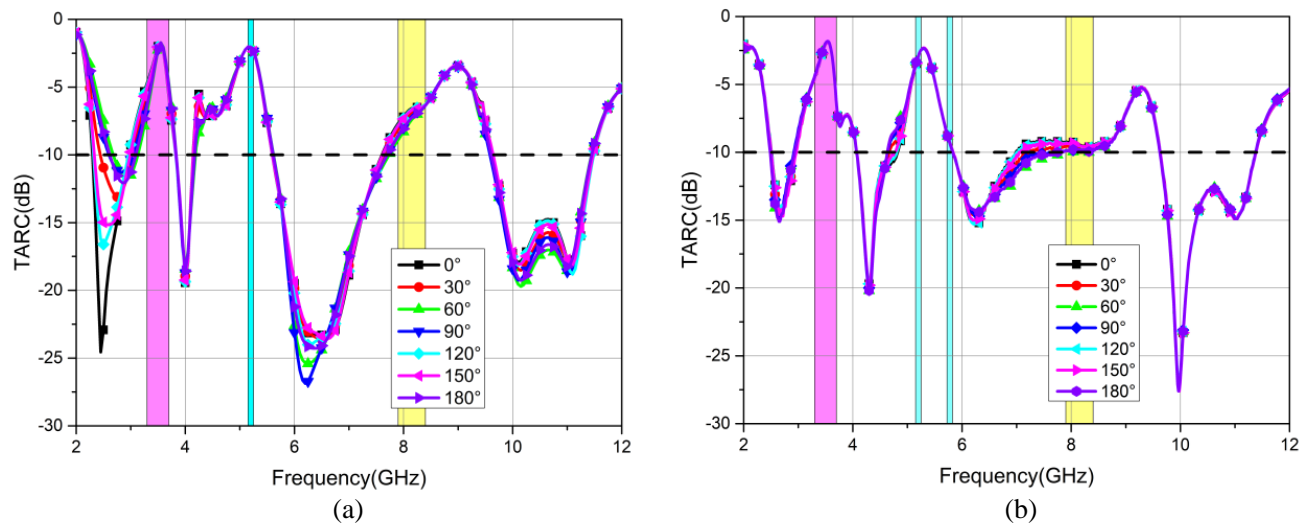
Figure 15. TARC of the MIMO antenna. (a) Simulated TARC. (b) Measured TARC.

5. CONCLUSION

A 4-element CPW-fed UWB MIMO slot antenna with triple band-notched characteristics is proposed. It has an overall size of $65\,\text{mm} \times 65\,\text{mm} \times 0.8\,\text{mm}$. To obtain high isolation, four antenna elements are placed vertically, and cross-shaped branches are added. The measured results demonstrate that the antenna covers 2.51–$11.07\,\text{GHz}$ with the isolation less than $-21\,\text{dB}$, and WiMAX, WLAN, and X-band interference is successfully suppressed. Measured and simulated results indicate that the designed antenna has great radiation performance, high isolation, low ECC, and sound gain in operating band.

REFERENCES

1. Tang, Z., X. Wu, J. Zhan, Z. Xi, and S. Hu, "A novel miniaturized antenna with multiple band-notched characteristics for UWB communication applications," *Electromagn. Waves Appl.*, Vol. 32, No. 15, 1961–1972, Jun. 2018.

2. Gautam, S. and K. Cecil, "A four-element planar UWB-MIMO antenna system comprising of plus-sign stub for high isolation," *Int. J. Eng. Adv. Technol.*, Vol. 7, 17–20, 2018.

3. Khan, M. S., A. D. Capobianco, S. Asif, et al., "A 4 element compact ultra-wideband MIMO antenna array," *IEEE Antennas Propag. Soc. AP-S Int. Symp.*, Vol. 2015, 2305–2306, 2015.

4. Palniladevi, M. P., "Compact MIMO Yagi-Uda antenna with parasitic strip for LTE application," *Int. J. Pure Appl. Math.*, Vol. 119, 1913–1919, 2018.

5. Biswal, S. P. and S. Das, "A low-profile dual port UWB-MIMO/diversity antenna with band rejection ability," *Int. J. RF. Microw. Comput.-Aided Eng.*, Vol. 28, No. 1, Art. no. e21159, Jan. 2017.

6. Liu, Y. Y. and Z. H. Tu, "Compact differential band-notched stepped-slot UWB-MIMO antenna with common-mode suppression," *IEEE Antennas Wireless Propag. Lett.*, Vol. 16, 593–595, 2017.

7. See, T. P. and Z. N. Chen, "An ultrawideband diversity antenna," *IEEE Trans. Antennas Propag.*, Vol. 57, No. 6, Jun. 2009.

8. Liu, Y. C., G. Zhe, and X. Shu, "Triple band-notched aperture UWB antenna using hollow-cross-loop resonator," *Electronics Letters*, Vol. 50, No. 10, 728–730, 2014.

9. Kang, L., H. Li, X. Wang, and X. Shi, "Compact offset microstrip-fed MIMO antenna for band-notched UWB applications," *IEEE Antennas Wireless Propag. Lett.*, Vol. 14, 1754–1757, 2015.

10. Bhattacharjee, A., A. Karmakar, A. Saha, and D. Bhattacharya, "Design of a compact UWB MIMO-diversity antenna incorporating fractal inspired isolation structure with band notch characteristics," *Microwave and Optical Technology Letters*, 2021.

11. Srivastava, G. and B. K. Kanuijia, "Compact dual band-notched UWB MIMO antenna with shared radiator," *Microwave and Optical Technology Letters*, Vol. 57, No. 12, 2886–2891, 2015.

12. Zhou, J.-Y., Y. Wang, J.-M. Xu, and C. Du, "A CPW-fed UWB-MIMO antenna with high isolation and dual band-notched characteristic," *Progress In Electromagnetics Research M*, Vol. 102, 27–37, 2021.

13. Jaglan, N., S. D. Gupta, E. Thakur, D. Kumar, B. K. Kanaujia, and S. Srivastava, "Triple band notched mushroom and uniplanar EBG structures based UWB MIMO/diversity antenna with enhanced wide band isolation," *AEU — International Journal of Electronics and Communications*, Vol. 90, 36–44, 2018.

14. Naktong, W. and A. Ruengwaree, "Four-port rectangular monopole antenna for UWB-MIMO applications," *Progress In Electromagnetics Research B*, Vol. 87, 19–38, 2020.

15. Tripathi, S., A. Mohan, and S. Yadav, "A compact Koch fractal UWB MIMO antenna with WLAN band-rejection," *IEEE Antennas Wireless Propag. Lett.*, Vol. 14, 1565–1568, 2015.

16. Raheja, D. K., B. K. Kanaujia, and S. Kumar, "Compact four-port MIMO antenna on slotted-edge substrate with dual-band rejection characteristics," *International Journal of RF and Microwave Computer-Aided Engineering*, e21756, 2019.

17. Muzaffar, K. and M. Idrees Magray, "Compact four element dual band notched orthogonally placed UWB antennas for wireless MIMO applications," *IEEE-APS Topical Conference on Antennas and Propagation in Wireless Communications (APWC)*, 285–287, Granada, Spain, 2019.

18. Tang, Z., X. Wu, J. Zhan, S. Hu, Z. Xi, and Y. Liu, "Compact UWB-MIMO antenna with high isolation and triple band-notched characteristics," *IEEE Access*, Vol. 7, 19856–19865, 2019.

19. Khaleel, H., H. Al-Rizzo, D. Rucker, and S. Mohan, "A compact polyimide-based UWB antenna for flexible electronics," *IEEE Antennas Wireless Propag. Lett.*, Vol. 11, 564–567, 2012.

20. Blanch, S., J. Romeu, and I. Corbella, "Exact representation of antenna system diversity performance from input parameter description," *Electron. Lett.*, Vol. 39, No. 9, 705–707, May 2003.

21. Tian, R., B. K. Lau, and Z. Ying, "Multiplexing efficiency of MIMO antennas," *IEEE Antennas Wireless Propag. Lett.*, Vol. 10, 183–186, 2011.

22. Karaboikis, M., V. Papamichael, G. Tsachtsiris, C. Soras, and V. Makios, "Integrating compact printed antennas onto small diversity/MIMO terminals," *IEEE Trans. Antennas Propag.*, Vol. 56, No. 7, 2067–2078, Jul. 2008.

23. Pandit S., A. Mohan, and P. Ray, "A compact four-element MIMO antenna for WLAN applications," *Microwave and Optical Technology Letters*, Vol. 60, 289–295, 2018.